ORIGINAL PAPER

The Positive Influence of Therapeutic Agent on Relaxivities of Gadolinium-Loaded Liposomal Theranostics

Beata Wereszczyńska[1,2,3] ⬦ · **Tomasz Zalewski**[2] ⬦

Abstract

This study investigates changes in the MRI contrast properties of Gd(III)-containing paramagnetic liposomes following the incorporation of photosensitizing agent (ZnPc—zinc phthalocyanine). It provides identification of mechanisms responsible for enhancement of proton relaxation rate and hence, the increased both r_1 and r_2 relaxivities. Five liposomal formulations, containing fatty acids derivatives of Gd(III) salt and hydrophobic ZnPc, were synthesized. NMRD profiles of liposomal solutions (magnetic field range from 0.0002 to 9.4 T) were obtained and Modified Florence model was applied. The contrast properties of the model drug itself was separated from the lipid bilayer deformation influence, caused by its incorporation. The latter resulted, among other, in optimization of an apparent water exchange correlation time. As Gd(III) is located in the outer and inner lipid layers, some of the Gd(III) chelates are localized in aqueous interior of the liposomes, thus their contrasting efficiency depends on the water exchange rate through the membrane. The proposed approach raises the possibility of reducing the amount of potentially harmful contrast media based on gadolinium, by taking into account the increase of the relaxation effect caused by other components of the system.

1 Introduction

The development of nanostructures that act simultaneously as contrast agents in imaging techniques and as carriers of therapeutic agents represents a challenge for nanotechnology. Using one substance, fulfilling the role of the two pharmaceuticals that are used for different purposes, enables combination of diagnostic and

✉ Beata Wereszczyńska
  b.wereszczynska@leeds.ac.uk

1   Department of Macromolecular Physics, Faculty of Physics, Adam Mickiewicz University, Poznan, Poland

2   NanoBioMedical Centre, Adam Mickiewicz University, Poznan, Poland

3   Leeds Institute of Cardiovascular and Metabolic Medicine, University of Leeds, Leeds, UK

treatment procedures and reduction of the patients' discomfort [1, 2]. One of the main problems for this type of system is the interaction between the contrast component and the therapeutically active agent. Proposed combination of zinc phthalocyanine (ZnPc—a model photosensitizer with extensive photochemical characterization in the literature, commonly tested in liposomal formulations [3–5]) and liposome's containing gadolinium $3+$(Gd(III)) (contrast agent for MRI) fits into idea of theranostic particles combining diagnostic and therapeutic function.

1.1 MRI Contrast Agents

MRI plays important role in medical diagnostics since it allows non-invasive visualization of tissues. Despite the extensive image contrast manipulation options provided by e.g., acquisition parameters changes, the ability to report specific pathophysiological processes is still limited. To improve image contrast ratio, MRI contrast agents (CAs) are being used which allow the acquisition of images where a greater number of pathological changes can be seen. CAs are not a source of the NMR signal, so themselves are invisible in MRI experiments. Their function is to change the magnetic properties of the environment in which they are located. This directly influences the relaxation processes, and thus, changes the T_1 and T_2 relaxation times. Nowadays, clinical applications employ mostly paramagnetic gadolinium ion chelates e.g., derivatives of pantothenic acid, i.e., Gd-DTPA (DTPA—diethylene triamine pentaacetic acid). These substances shorten both longitudinal relaxation time (T_1) and transverse relaxation time (T_2) of surrounding water protons, which result in changes of the specified area signal intensity, thereby increasing contrast between areas in the MRI image. T_1 and T_2 relaxation times in presence of contrast agent depend on concentration of the agent and its contrasting efficiency characterized by longitudinal and transverse relaxivity (r_1, r_2) [6, 7] defined as follows:

$$\frac{1}{T_{i(obs)}} = r_i C + \frac{1}{T_i}, \, i = 1 \, or \, 2. \tag{1}$$

where $T_{i(obs)}$ is a relaxation time of the aqueous system, r_i – relaxivity, C – the concentration of the CA, and T_i – relaxation time of the system before addition of the CA. Relaxivity can be also defined as the increase of relaxation, produced by 1 mmol per litre of CA.

1.2 Liposomes as MRI CA

Liposomes are versatile nanoparticles of modifiable physical and chemical properties [8]. The amphiphilicity of lipids, which allow the transfer of both hydrophilic and hydrophobic substances in a biocompatible carrier, open the way to a plethora of applications. There are numerous examples of their use as drug carriers e.g. in cancer treatment [8–11]. The range of liposomes applications has been expanded by the incorporation of gadolinium in their structure, converting them into paramagnetic systems useful as MRI contrast agent [12–14]. The insertion of gadolinium in liposomes paved the way to construct multimodal particles with joined diagnostic

and therapeutic function. Taking into account a wide range of currently available types of lipids, there is a large number of possible liposome compositions with various physicochemical properties [8, 14]. Paramagnetic liposomes intended for use in MRI are obtained either by placing a hydrophilic gadolinium chelate in the aqueous lumen of a liposome [8], or through the incorporation of gadolinium-functionalized amphiphilic lipids in the lipid bilayer [8, 12–14]. In the first case, the relaxation effect is clearly visible only after increasing the permeability of the lipid membrane at nanoparticles destination site. Use of the second method results in a time constant relaxation effect depending on the amount of Gd (III) incorporated into the outer lipid layer (strong effect on the water protons relaxation rate) and inner lipid layer (relaxation effect limited by lipid membrane permeability). It should also be noted that an increase in popularity of paramagnetic liposomes containing therapeutic substances (so-called Theranostic agents) is reported [8]. These particles allow the simultaneous assessment of the biodistribution of drugs administered to the body and of their therapeutic efficacy. Observation as therapeutics propagate in the body is possible using T_1-weighted MRI scans [10].

To explain contrasting efficiency of paramagnetic CA, relaxation models based on Salomon–Bloembergen–Morgan (SBM) and Freed theories are used [15]. According to the literature, for systems with the size of the investigated liposomes (about 130 nm), the most suitable is modified Florence approach [16] that contains appropriate corrections (i.e., for slowly rotating systems (big particles); zero field splitting (ZFS—interactions of the energy levels of an electron spin S > 1/2); hyperfine interaction between the electron spin and the nucleus of the paramagnetic ion; electronic g-factor anisotropy). It should be noted, that the model does not actually consider exact size of the particles. Modified Florence approach enables interpretation of NMRD (Nuclear Magnetic Relaxation Dispersion) profiles of paramagnetic liposomes [17] and comparison of calculated parameters (e.g., proton-paramagnetic ion distance—r, water residence time—τ_M, rotational correlation time—τ_R (Fig. 1), correlation time of electron relaxation—τ_V and ZFS parameters) allows to determine the physical basis of the observed relaxation.

1.3 ZnPc-Gd(III) Liposomal Theranostics

Biological studies performed in the frame of our previous work provided information on the temporal stability, sizes, biocompatibility and satisfactory therapeutic efficacy and safety of use of this kind of system [14]. This work is focused on the explanation of the influence of ZnPc incorporation on the contrasting properties of bimodal paramagnetic liposomes, that were described in our previous article [14]. Different liposomal formulations with MRI CA functionality (by the content of lipid derivative of gadolinium(III) diethylenetriamine pentaacetic acid salt) and therapeutic functionality for photodynamic therapy of cancer (by the content of ZnPc) were investigated. Such liposomes exhibit constant contrasting properties regardless of the stage of the medical procedure, allowing tracing of the therapeutic substance in the body and obtaining well-contrasted MRI images of the treated tissues before and after single step of the treatment. As shown before [14], all tested liposomal formulations had higher
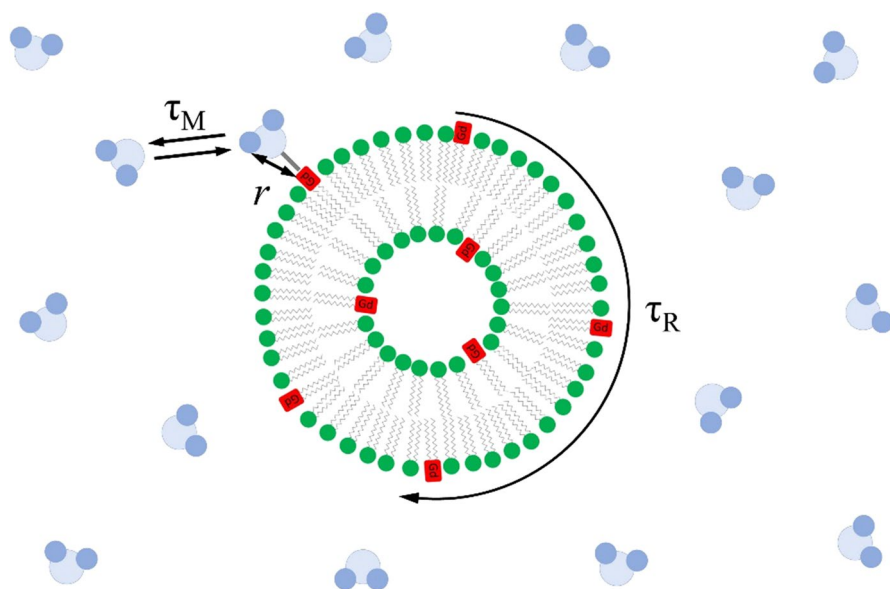
Fig. 1 Relaxation theory parameters: water residence time -τ_R, rotational correlation time—τ_M and proton-paramagnetic ion distance—r

relaxivities than those of commercially used CAs. The incorporation of ZnPc into the liposomes increased the relaxation parameters r_1 and r_2, in comparison to the values for non-loaded ones [14]. Investigation of relaxation properties of ZnPc in water solution is not possible because of its strong hydrophobicity. The incorporation of ZnPc into the lipid bilayer enables it to propagate in aqueous media and hence it is possible to explore its relaxation properties within liposomes. On the other hand, contrast agents based on Gd(III), due to the paramagnetism of gadolinium ion, are widely used in diagnostic imaging. Undoubtfully, Gd(III) is a representative of toxic heavy metals family and forms a few temporarily stable chelates only in the presence of suitable ligand (e.g., DTPA) [18]. Work on the reduction of an amount of Gd(III) in therapeutic formulations, that would subsequently minimize the risk of side effects associated with its toxicity, is still in progress and currently a big challenge. According to our knowledge, there are no other literature reports than our previous work [14], about drug molecules impacting the relaxation properties of paramagnetic liposomes. In this work, we show that consideration of this effect may result in achieving planned contrasting efficiency with reduced amount of Gd(III) in the formulation.

2 Materials and Methods

2.1 Liposome Preparation

The liposomes (Fig. 2) are composed of commercially available fatty acids derivatives of Gd(III) salt (bis(1,2-dipalmitoyl-*sn*-glycero-3-phosphoethanolamine)-

N–N'-diethylenetriaminepentaacetic acid (gadolinium salt), Gd-DTPA2) and POPC (1-palmitoyl-2-oleoyl-sn-glycero-3-phosphocholine) and PG (1-palmitoyl-2-oleoyl-sn-glycero-3-phosphate) as basic phospholipids of liposomal membrane. Incorporation of the Gd (III) in the form of lipid derivative ensures the spontaneous incorporation of all Gd into the structure of the forming nanoparticles. Hydrophobic (and, therefore, not dispersible in aqueous media) photosensitizing agent ZnPc is also incorporated into the lipid bilayer. Liposomes were prepared by a thin-film hydration method [14]. Solutions of lipids and ZnPc in chloroform were mixed and evaporated under reduced pressure. The resulting film was hydrated with physiological saline and dispersed by vortexing for 10 min. The liposome suspension was passed through polycarbonate membranes to achieve a uniform size distribution. Five liposomal formulations were synthesized. Molar ratios of liposomal components (Gd-DTPA2: POPC: PG: ZnPc) were: 0.75: 8: 2: 0 (0.75Gd-lip); 0.75: 8: 2: 0.1 (0.75Gd-ZnPc-lip); 0.03: 8: 2: 0 (0.03Gd-lip); 0.03: 8: 2: 0.1 (0.03Gd-ZnPc-lip); 0: 8: 2: 0.1 (ZnPc-lip).

2.2 NMR Relaxometry

Proton T_1 relaxation times have been measured for five samples of known concentrations for every liposomal formulation in physiological saline using Inversion Recovery pulse sequence or balanced non-polarized or pre-polarized FFC sequence. The study of longitudinal relaxation dispersion has been carried out using NMR spectrometers with magnetic field strength of 9.4 T (Agilent MRI scanner), 4.7 T
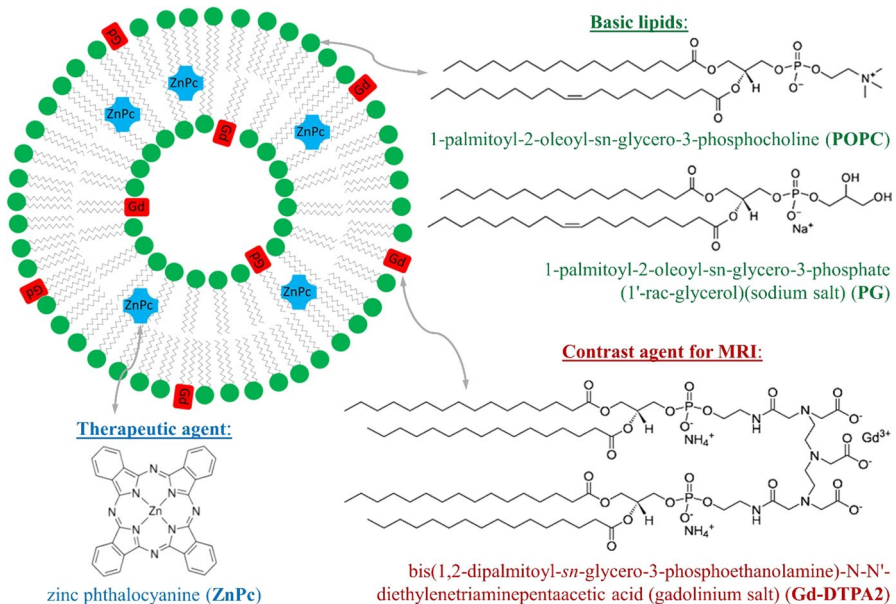

Fig. 2 Schematic structure of the analysed composite liposome nanoparticles

(Bruker CPX), 1.4 T (home built), 0.4 T (home built) and Fast Field Cycling (Stelar Spinmaster 2000) spectrometer with magnetic field range from 0.0002 to 0.3525 T. The transverse relaxation study (using CPMG pulse sequence) was conducted in 0.4 T and 9.4 T. The measurements were carried out at room temperature and 37 °C—corresponding to the temperature of human internal organs.

2.3 Analysis of Relaxation Profiles

Relaxivities r_1 have been calculated from obtained T_1 data for each type of liposomes in all magnetic field strengths. The achieved data were used to create NMRD profiles. Modified Florence approach was used to relaxation characterization using a program developed by Bertini et al. [16, 19].

3 Results

Obtained ^{1}H NMRD profiles are typical of Gd complexes bound to a macromolecule [20]. Maximal contrasting efficiency of studied nanoparticles falls about the range of magnetic fields used in diagnostics and achieved r_1 values make studied particles very efficient contrast agents for MRI. This effect is strongly reinforced in the case of liposomes with incorporated ZnPc (Fig. 3). To assess how much of this reinforcement originates just from ZnPc relaxometric properties, relaxation rates R_1 of ZnPc-lip were measured. Auxiliary profiles were created by subtracting ZnPc-lips' R_1 values from 0.75Gd-ZnPc-lips' and 0.03Gd-ZnPc-lips' (at high magnetic fields) R_1 values and calculating r_1 for this new datasets. It was impossible to calculate such a profile for 0.03Gd-ZnPc-lip at low magnetic fields as the relaxation effect induced by ZnPc-lip is comparable to the 0.03Gd-ZnPc-lip relaxation effect. In the case of 0.75Gd-ZnPc-lip, it is clear that after subtracting the ZnPc-lip influence, the calculated profile does not coincide with the 0.75Gd-lip NMRD profile, suggesting more complex nature of the observed relaxation increase. Also, there is no evidence in the literature to argue that incorporation of ZnPc forces Gd-containing lipid derivatives to be located more frequently in the outer lipid layer.

To achieve relaxation parameters, the modified Florence model was fitted to the experimental data. Proton-metal ion distance r was fixed at 3.1 Å according to the literature [18]. The best fit parameters are listed in Table 1. The height and position analyses of maximum r_1 peak were not implemented due to the interpolation uncertainty. Distance of the closest approach d was fixed during calculations on values from 3.60 (maximal outer sphere [17]) to 4.1 Å for every liposomal formulation. The best fits were obtained for 3.60 and 3.63 Å, what suggests relatively large outer sphere contribution. The τ_R values obtained from the theoretical fittings are assumed to be influenced by the local mobility of the Gd-DTPA2 as global rotational correlation time is expected to be orders of magnitude lower [17, 21]. As it was expected, τ_R shortening with rise of temperature was observed. Likewise, liposomes with greater amount of heavy Gd-DTPA2 lipids had longer τ_R, which was elongated even more by the incorporation of ZnPc.
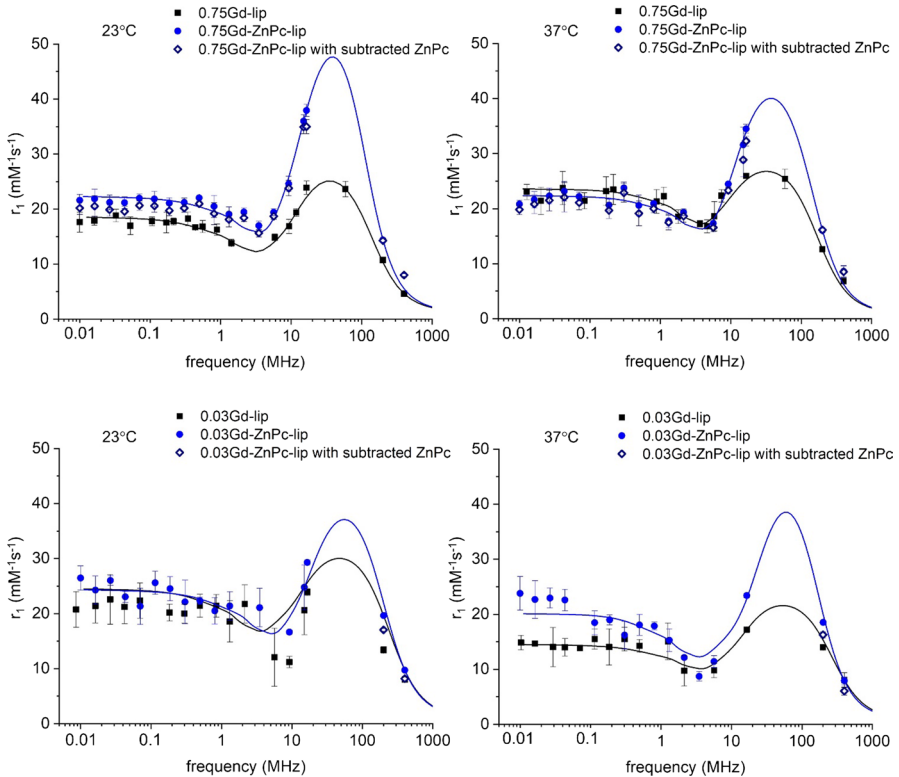
Fig. 3 NMRD profiles of liposomes 0.75Gd -lip, 0.75Gd-ZnPc-lip, 0.75Gd-ZnPc-lip with subtracted ZnPc influence, 0.03Gd-lip, 0.03Gd-ZnPc-lip and 0.03Gd-ZnPc-lip with subtracted ZnPc influence (where possible). The r_1 calculation was based on Gd(III) molar concentration

This effect is probably caused by increased average weight of the liposome. Electronic relaxation time τ_V values are close to 30 ps for liposomes without ZnPc as expected for Gd complexes. For liposomes containing ZnPc, there is a wide range of τ_V values calculated. The residence lifetime of the water molecule in the coordination site of the metal chelate τ_M has reasonable values comparing to the literature [17] and gets shorten with the rise of temperature and ZnPc incorporation. The axial component of ZFS D_{ZFS} values, similar as in the literature [17, 18], are about 0.03 cm^{-1} and increase with temperature and ZnPc incorporation (except for 0.03Gd-ZnPc-lip). The transient zero field splitting Δ_{ZFS} values are slightly bigger than in the literature of similar systems [17], mostly decrease with temperature and rise after ZnPc incorporation.

Results of transverse relaxivity study are listed in Table 2. Measurements at 16.5 MHz revealed T_2-weighted clinical imaging potential of analysed liposomes, as obtained r_2 values are from 12.78 up to 49.50 mM^{-1} s^{-1}. Values of r_2 achieved at 400 MHz (up to great number of 128.23 mM^{-1} s^{-1} for 0.75Gd-ZnPc-lip at room temperature) make all examined liposomal formulations a very promising CA for

Table 1 Best fit parameters for the NMRD data of studied liposomal formulations

best fit parameters	0.75Gd-lip 23 °C	0.75Gd-ZnPc-lip 23 °C	0.75Gd-lip 37 °C	0.75Gd-ZnPc-lip 37 °C	0.03Gd-lip 23 °C	0.03Gd-ZnPc-lip 23 °C	0.03Gd-lip 37 °C	0.03Gd-ZnPc-lip 37 °C
τ_R [10^{-9} s]	5.31	5.74	2.66	2.67	1.90	2.31	1.33	2.15
τ_V [10^{-12} s]	33.8	68.8	31.1	67.1	24.52	25.8	31.4	17.8
τ_M [10^{-6} s]	2.45	1.50	1.57	1.05	2.24	1.90	1.79	1.10
d [Å]	3.63	3.60	3.63	3.60	3.63	3.63	3.63	3.63
D_{ZFS} [10^{-2} cm^{-1}]	2.29	3.15	2.90	3.41	2.71	4.17	2.98	2.63
Δ_{ZFS} [10^{-2} cm^{-1}]	3.86	5.23	2.24	3.88	3.44	4.78	4.25	4.38

Table 2 r_2 of studied liposomal formulations (calculated value ± standard error)

Formulation	r_2 in 16,5 MHz [mM^{-1} s^{-1}]		r_2 in 400 MHz [mM^{-1} s^{-1}]	
	23 °C	37 °C	23 °C	37 °C
0.75Gd-lip	12.78 ± 0.72	21.52 ± 1.69	72.00 ± 3.50	75.15 ± 1.66
0.75Gd-ZnPc-lip	49.50 ± 3.71	42.56 ± 5.03	128.23 ± 3.12	101.59 ± 4.63
0.03Gd-lip	26.86 ± 2.79	22.60 ± 1.69	76.49 ± 2.02	57.78 ± 3.72
0.03Gd-ZnPc-lip	36.04 ± 0.87	29.55 ± 2.66	86.06 ± 3.22	66.71 ± 3.11
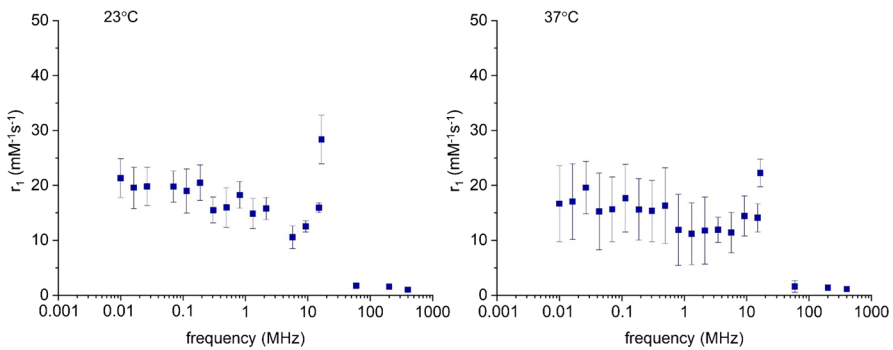
Fig. 4 NMRD profiles of ZnPc-lip. The r_1 calculation was based on ZnPc molar concentration at two different temperatures (23 ºC—on the left and 37 ºC—on the right)

preclinical imaging. In all cases, there was a significant r_2 increase caused by the incorporation of ZnPc into the lipid bilayer.

NMRD profiles of ZnPc-lip solutions are shown in Fig. 4. The shape of obtained profiles is surprising and not typical for a diamagnetic solution. The profiles resemble NMRDs of paramagnetic systems, so dipolar interactions between Gd (III) ions and ZnPc are not out of the question. The nature of magnetic properties of ZnPc-lip remains inconclusive, however, these are out of the scope of the current manuscript and will be investigated in future.

Detailed characterisation of this type of liposomes by means of differential scanning calorimetry (DSC), nanoparticle tracking analysis (NTA), transmission electron microscopy (TEM) as well as information about singlet oxygen production, photodynamic properties and in vitro cell viability were presented in our previous work [14].

4 Discussion and Conclusions

ZnPc is known as diamagnetic molecule, however, it has been shown that metallophthalocyanines can self-assemble to produce aggregates that exhibit ferromagnetism at room-temperature [22]. ZnPc does not form supramolecular aggregates [22], but it can form dimers and trimers [23, 24] which can substantiate non-zero relaxivities

of ZnPc-lip solution. Strong disagreement of 0.75Gd-lip and 0.75GdZnPc-lip with subtracted ZnPc-lip NMRD profiles leads to additional explanations of the observed phenomenon. Modified Florence model fitting provided a partial explanation as not all parameters calculated for ZnPc-containing liposomes were agreeing with expectations. ZnPc is placed in the hydrophobic part of the lipid bilayer and Gd(III) chelate remains in the hydrophilic part, so there is no reason to believe that ZnPc can affect water–CA bonding. Doubling of τ_V value and decrease of τ_M after ZnPc incorporation may originate from lack of other parameters that can efficiently enlarge inner sphere relaxation contribution related, e.g., to the change of lipid membrane permeability.

As Modified Florence approach is the most appropriate paramagnetic relaxation model for liposomal CA (according to the literature [16, 17]), an attempt of fitting improvement was made. The most common way to improve fitting results is to fix more parameters to known or reasonably estimated values. Some of the scientists are of the opinion that determination of τ_M from NMRD profile is disputable and the parameter should be fixed at value specific for the particular Gd(III)-chelate. However, literature shows, that this value varies significantly when different compounds are bound to the chelate. According to the literature, for Gd-DTPA-x τ_M is 230–2252 ns (lipid derivatives not listed) [18], for some of its lipid derivatives incorporated into the liposome, we can expect τ_M of 1100–2300 ns (data based on NMRD profiles) [17]. One could also think of fixing ZFS parameters on values obtained from EPR studies. For small complexes and low molecular weight chelates, the analysis of EPR measurements in aqueous solution provided parameters compatible with NMR relaxation data, however, for slow-rotating molecules, calculations of liquid solution EPR lines get too complex and computationally expensive so to get proper data solid-state EPR method should be used. Unfortunately, it was shown that transient ZFS strength and second order static ZFS strength determined by EPR are significantly different for aqueous solution, frozen solution and powder of the Gd-DTPA [25, 26]. Hence, axial component of ZFS D_{ZFS} and rhombic component of ZFS E_{ZFS} (possible to calculate from solid-state EPR spectra) are different for frozen solution and powder and can also be considered different from those occurring in a liquid solution. D_{ZFS} for $[Gd(DTPA)(H_2O)]^{2-}$ are -0.029 cm^{-1} (powder) and 0.048 cm^{-1} (frozen); E_{ZFS} are 0.004 cm^{-1} (powder) and 0.013 cm^{-1} (frozen) [25, 26]. It was concluded that results obtained for frozen solutions are more appropriate to determine accurately ZFS parameters for MRI CA [25], but still the specific values were not given.

The attempt to include E_{ZFS} to fitting procedure was made, but it did not improve fits and resulted in significant lengthening of one profile calculation time, therefore we abandoned this approach. According to the literature describing liposomes with lipid derivatives of Gd-DTPA, D_{ZFS} is 0.02—0.03 cm^{-1}, Δ_{ZFS} is 0.010–0.024 cm^{-1} and E_{ZFS} is not implemented to the model [17]. Correlation time of electron relaxation τ_V for Gd-DTPA-x is 3—60 ps [18] and for some of its lipid derivatives in liposomes 19—30 ps [17].

In general, best fit parameters obtained in this study are in good agreement with literature data, so it can be assumed that they reflect reality, but they can also be postulated as apparent values since applied model does not comprise parameter

describing additional liposomal membrane characteristics. One of those affecting relaxivity features can be water permeability of the lipid bilayer. In case of presented liposomes, Gd-DTPA2 is located in the outer and inner layers, so some of the Gd(III) chelates are localized in aqueous interior of the vesicles and their contrasting efficiency depends on the water exchange rate through the membrane [21]. It should be noted, that mentioned rate affect "global" water exchange rate that can be observed as changes of τ_M [21]. In this context fitting parameter, τ_M can be considered not as the residence lifetime of the water molecule in the coordination site of the metal chelate but "mixed" water exchange correlation time. Therefore, decrease of τ_M, observed after ZnPc incorporation in this study might suggest increase of water permeability of the membrane due to locally incompact structure of the bilayer. Such structure modification may result in larger mobility of lipids, including Gd(III) lipid derivatives, and increased flexibility/deformability of the membrane. The latter is associated with transient ZFS Δ_{ZFS}, what explains increase of its value when ZnPc incorporated. However, reasoning about liposome flexibility based on Δ_{ZFS} is not practiced in the literature, to our knowledge. Additional measurements, such as dynamic light scattering or cryo-electron microscopy could also be helpful in final assessment of liposomes' structure.

There is a FFC-based method of determination of bending elastic modulus in liposome membranes, but it is based on NMR relaxation of lipid-building protons, not the protons of the solvent and it is characterized by a completely different approach [27]. Transverse relaxivity r_2 were obtained only in two magnetic field strengths, so they do not create the possibility of fitting any relaxation model. However, for a model that was the antecedent of modified Florence approach, Bertini et al. presented calculations of T_2 as almost analogous to T_1 [28], so consistent increase of r_2 after ZnPc incorporation is in line with our expectations.

Enhancement of the relaxivity of paramagnetic liposomes caused by the incorporation of ZnPc leads the way to reduction of the dose of potentially harmful Gd(III) in novel type of bimodal liposomes combining diagnostic (MRI CA) and therapeutic (photodynamic therapy of cancer) function. Understanding this phenomenon is crucial for future development of safest and more efficient anticancer-MRI theranostics. It seems that the effect originates mainly from liposome membrane structure modification. Modified Florence model fitting results in combination with literature data, focused the attention on the lipid bilayer water permeability and deformability changes that occur as a result of ZnPc incorporation.

Author Contributions Study conception and design: BW and TZ. Data collection, data analysis, data visualization and drafting of manuscript: BW. Critical revision: TZ.

Data Availability The datasets generated during the current study are available from the corresponding author on reasonable request.

Compliance with Ethical Standards

References

1. J.V. Jokerst, S.S. Gambhir, Acc. Chem. Res. **44**, 1050–1060 (2011). https://doi.org/10.1021/ar200106e
2. J.H. Ryu, S. Lee, S. Son, S.H. Kim, J.F. Leary, K. Choi, I.C. Kwon, J. Control. Release **190**, 477–484 (2014). https://doi.org/10.1016/j.jconrel.2014.04.027
3. H.L. van Leengoed, V. Cuomo, A.A. Versteeg, N. van der Veen, G. Jori, W.M. Star, Br. J. Cancer **69**, 840–845 (1994). https://www.ncbi.nlm.nih.gov/pubmed/8180012.
4. U. Isele, K. Schieweck, P. van Hoogevest, H.-G. Capraro, R. Kessler, J. Pharm. Sci. **84**, 166–173 (1995). https://doi.org/10.1002/jps.2600840209
5. D.S. Maranho, R.G. De Lima, F.L. Primo, R.S. Da Silva, A.C. Tedesco, Photochem. Photobiol. **85**, 705–713 (2009). https://doi.org/10.1111/j.1751-1097.2008.00481.x
6. R.B. Lauffer, Chem. Rev. **87**, 901–927 (1987). https://doi.org/10.1021/cr00081a003
7. E.J. Werner, A. Datta, C.J. Jocher, K.N. Raymond, Angew. Chem. Int. Ed. Engl. **47**, 8568–8580 (2008). https://doi.org/10.1002/anie.200800212
8. S. Langereis, T. Geelen, H. Grull, G.J. Strijkers, K. Nicolay, NMR Biomed. **26**, 728–744 (2013). https://doi.org/10.1002/nbm.2971
9. D.C. Drummond, C.O. Noble, M.E. Hayes, J.W. Park, D.B. Kirpotin, J. Pharm. Sci. **97**, 4696–4740 (2008). https://doi.org/10.1002/jps.21358
10. M.E. Lobatto, Z.A. Fayad, S. Silvera, E. Vucic, C. Calcagno, V. Mani, S.D. Dickson, K. Nicolay, M. Banciu, R.M. Schiffelers, J.M. Metselaar, L. van Bloois, H.S. Wu, J.T. Fallon, J.H. Rudd, V. Fuster, E.A. Fisher, G. Storm, W.J. Mulder, Mol. Pharm. **7**, 2020–2029 (2010). https://doi.org/10.1021/mp100309y
11. V.P. Torchilin, Nat. Rev. Drug Discov. **4**, 145 (2005). https://doi.org/10.1038/nrd1632
12. T. Geelen, L.E. Paulis, B.F. Coolen, K. Nicolay, G.J. Strijkers, Contrast Med. Mol. Imaging **8**, 117–126 (2013). https://doi.org/10.1002/cmmi.1501
13. L.E. Paulis, T. Geelen, M.T. Kuhlmann, B.F. Coolen, M. Schafers, K. Nicolay, G.J. Strijkers, J. Control. Release **162**, 276–285 (2012). https://doi.org/10.1016/j.jconrel.2012.06.035
14. P. Skupin-Mrugalska, L. Sobotta, A. Warowicka, B. Wereszczynska, T. Zalewski, P. Gierlich, M. Jarek, G. Nowaczyk, M. Kempka, J. Gapinski, S. Jurga, J. Mielcarek, J. Inorg. Biochem. (2018). https://doi.org/10.1016/j.jinorgbio.2017.11.025
15. L. Helm, Prog. Nucl. Magn. Reson. Spectrosc. **49**, 45–64 (2006). https://doi.org/10.1016/j.pnmrs.2006.03.003
16. D. Kruk, T. Nilsson, J. Kowalewski, Phys. Chem. Phys. **3**, 4907–4917 (2001). https://doi.org/10.1039/B106659P
17. F. Alhaique, I. Bertini, M. Fragai, M. Carafa, C. Luchinat, G. Parigi, Inorg. Chim. Acta **331**, 151–157 (2002). https://doi.org/10.1016/S0020-1693(01)00779-4
18. P. Caravan, J.J. Ellison, T.J. McMurry, R.B. Lauffer, Chem. Rev. **99**, 2293–2352 (1999). https://doi.org/10.1021/cr980440x

19. I. Bertini, J. Kowalewski, C. Luchinat, T. Nilsson, G. Parigi, J. Chem. Phys. **111**, 5795–5807 (1999). https://doi.org/10.1063/1.479876
20. S. Aime, M. Botta, M. Fasano, E. Terreno, Chem. Soc. Rev. **27**, 19–29 (1998). https://doi.org/10.1039/A827019Z
21. S. Laurent, L. Vander Elst, C. Thirifays, R.N. Muller, Eur. Biophys. J. **37**, 1007–1014 (2008)
22. B. Dhara, P.K. Jha, K. Gupta, V.K. Bind, N. Ballav, J. Phys. Chem. C **121**, 12159–12167 (2017). https://doi.org/10.1021/acs.jpcc.7b02145
23. T.G. Gantchev, J.E. van Lier, D.J. Hunting, Radiat. Phys. Chem. **72**, 367–379 (2005). https://doi.org/10.1016/j.radphyschem.2004.06.012
24. L.T. Ueno, A.E.H. Machado, F.B.C. Machado, J. Mol. Struct. Theochem. **899**, 71–78 (2009)
25. M. Benmelouka, Ph.D. Thesis, École Polytechnique Fédérale Lausanne, Lausanne, Switzerland (2006). https://doi.org/10.5075/epfl-thesis-3467
26. M. Benmelouka, J. Van Tol, A. Borel, M. Port, L. Helm, L.C. Brunel, A.E. Merbach, J. Am. Chem. Soc. **128**, 7807–7816 (2006). https://doi.org/10.1021/ja0583261
27. G.A. Dominguez, J. Perlo, C.C. Fraenza, E. Anoardo, Chem. Phys. Lipids **201**, 21–27 (2016). https://doi.org/10.1016/j.chemphyslip.2016.10.006
28. I. Bertini, O. Galas, C. Luchinat, G. Parigi, J. Magn. Reson. Ser. A **113**, 151–158 (1995). https://doi.org/10.1006/jmra.1995.1074